Contract No.:

This manuscript has been authored by Savannah River Nuclear Solutions (SRNS), LLC under Contract No. DE-AC09-08SR22470 with the U.S. Department of Energy (DOE) Office of Environmental Management (EM).

Disclaimer:

This document was prepared in conjunction with work accomplished under Contract No. DE-AC09-08SR22470 with the U.S. Department of Energy (DOE) Office of Environmental Management (EM).

Derivation of the Structural Integrity of Residual (SIR) Glass Model for the Enhancement of Waste Loading

Devon L. McClane[1,*], Jake W. Amoroso[1], Madison C. Hsieh[1], Kevin M. Fox[1], Albert A. Kruger[2]

[1]Savannah River National Laboratory, 227 Gateway Dr., 999-W, Aiken, SC 29803, USA
[2]U.S. Department of Energy, Office of River Protection, P.O. Box 450, MSIN H6-60, Richland, WA 99352, USA

[*]Corresponding Author E-mail address: Devon.Mcclane@srnl.doe.gov

Abstract

A new model based on glass structure to allow for enhanced waste loading in nuclear waste glass while maintaining chemical durability is proposed. The model is derived by splitting the molar concentrations of the targeted starting glass composition into theoretical crystalline phases anticipated to be observed during devitrification and a residual glass. An empirically derived relationship based on maintaining the residual glass structure, determined from a calculated non-bridging oxygen content, was demonstrated to successfully screen glasses for acceptable durability. The proposed model can successfully identify durable glass compositions containing 20-35 wt% Al_2O_3, a concentration that would significantly increase the projected waste loading in glasses processed at the Hanford Tank Waste Treatment and Immobilization Plant.

1 Introduction

The United States Department of Energy (DOE) Office of River Protection (ORP) plans to process ~200-million liters of radioactive waste through the Hanford Tank Waste Treatment and Immobilization Plant (WTP), a task anticipated to require ~50 years and cost over $100 billion(1). Wastes to be processed in this facility will include high concentrations of Na_2O(2) and/or high concentrations of Al_2O_3(3). When processed together, waste loading in glasses prepared from these streams is primarily limited by the formation of nepheline ($NaAlSiO_4$) crystals during slow cooling in the canisters(3). Nepheline crystallization is of primary concern due to its association with a deleterious change in the chemical durability of waste glasses(4, 5).

To prevent the formation of this detrimental crystalline phase, a Nepheline Discriminator (ND) developed around the relative mass ratios of Na_2O, Al_2O_3, and SiO_2, shown in Equation 1, has been employed(6-8). Despite the effectiveness of this discriminator, it can also unnecessarily restrict access to glass composition regions and limit waste loading. Since an increase in waste loading leads to a shorter mission and reduced life-cycle costs, there have been several recent studies focused on developing new methods to identify glass composition regions that allow for an increase in waste loading while maintaining a resistance to undesirable crystal formation. Some of these methods include: the Optical Basicity (OB) model which focuses on calculating the basicity of the cations, the Neural Network

(NN) model which was developed to incorporate complex non-linear interactions, the Sub-Mixture model (SM) which applies a polynomial fit to a pseudo-ternary diagram, and the Difference based on Correlation (DC) descriptor which combined the differences between the mass fractions of oxides observed to have positive and negative association with nepheline formation(9-12). While these techniques have generally resulted in incremental advances needed to successfully increase the concentration (i.e. waste loading) of Al_2O_3 in the resulting waste glass, several shortcomings still exist. These techniques are largely computationally based, rely on absolute glass composition inputs (wt%), don't necessarily consider how changes between component ratios influence the glass structure, and focus solely on circumventing crystallization instead of maintaining glass durability. Therefore; a new method to predict durable glasses with higher alumina concentrations is still desirable.

$$ND = \frac{SiO_2}{Na_2O + Al_2O_3 + SiO_2} \geq 0.62 \qquad (1)$$

A recent study investigating changes to glass durability as a function of the degree of nepheline crystallization revealed a strong correlation between the measured elemental release from a glass and the connectivity of its residual glass structure(13). Results from this study indicated two new strategies for allowing an increase in Al_2O_3 waste loading while ensuring the glass maintains an acceptable durability may be viable. The first strategy is dependent on controlling the nucleation and crystal growth behavior so that nepheline preferentially forms at the surface (i.e., the glass in contact with the canister wall). The second strategy is dependent on ensuring the residual glass, post-crystallization, maintains its structural integrity and chemical durability. This study focuses on the latter strategy to develop a new model, henceforth referred to as the Structural Integrity of Residual or "SIR" model, based on glass structure to improve waste loading while maintaining glass durability.

2 Experimental Procedures

2.1 Glass Composition Selection

Waste streams anticipated to be processed in the Hanford site have been categorized by the anticipated glass-limiting components for vitrification. One of the largest of these categories, including approximately 47 wt% of the high level waste, is waste which is limited by the quantity of Al_2O_3(3). Representative compositions of the Al_2O_3 and Al_2O_3/Na_2O limited waste streams(14) are shown in Table 1. These compositions were used to select the concentration and chemical makeup of the minor species included in a set of 50 non-radioactive test glasses formulated for the present study by targeting a 36 wt% waste loading (the concentration of waste in the final glass waste form currently targeted at the Defense Waste Processing Facility(15)). All components with a concentration greater than $1.5x10^{-5}$

moles/gram of glass were included. In addition to these minor components, Li_2O was included at a set concentration of 4 wt% for all test glasses. Since one of the objectives of this study was to investigate the effects caused by varying the ratios between the four major glass components (Al_2O_3, B_2O_3, Na_2O, and SiO_2), the relative concentration of the minor components was held fixed. The ratios between the remaining major components (Al_2O_3, B_2O_3, Na_2O, and SiO_2), constituting 85.2 wt% of the glass, were varied to fill the ternary diagrams shown in Figure 1. All test glasses were formulated to challenge the Nepheline Discriminator, with values ranging between 0.31 and 0.59, in an attempt to identify a glass forming region that would allow for an increase in Al_2O_3 waste loading. Targeted concentrations of the minor and major component oxides in the 50 test glasses are summarized in Table 1 and listed individually in Table S1 in supplemental data. The total concentrations of the major components (wt%) are displayed in a scatter plot matrix, Figure 2, to highlight the compositional breadth and distribution of the studied glass compositions.

2.2 Glass Processing and Heat Treatment

Fifty-gram glass batches were prepared by manually mixing stochiometric amounts of reagent grade oxides, carbonates, sulfates, phosphates, boric acid, and sodium fluoride. Batches were heated from ambient temperature to 1200°C in covered Pt-10Rh crucibles, isothermally held for approximately one hour, and water-quenched. The resulting glasses were ground using an Angstrom TE250 Ring Pulverizer with tungsten carbide grinding container (Angstrom, Inc., Belleville, MI). Twenty-five grams of each quenched and ground glass was loaded into a covered 30-mL Pt-5Au crucible and placed in a pre-heated Thermolyne 48000 furnace (Thermo Fisher Scientific, Waltham, MA) for heat treatment. Glasses were initially held at 1200°C for approximately one hour to remove any influences from the initial melt and quench, then cooled at a rate of 20°C/min to 1000°C, isothermally held for 5 min, and finally cooled at a rate of 0.5°C/min to 400°C, at which point the furnace power was turned off and the glass was allowed to cool to room temperature. As shown in a recent paper(13), this heat treatment is expected to be similar to, and produce crystallization prototypic of, that seen in a bulk glass during canister cooling.

2.3 Glass Analysis

Heat treated glasses were sectioned using a Buehler Isomet™ low speed saw (Buehler, Lake Bluff, IL) with diamond wafering blade. Glasses were subsequently polished using an Allied Multiprep™ precision polishing system (Allied High-Tech Products, Inc., Rancho Dominguez, CA) and imaged to categorize the observed crystalline phases. Images were produced using a Hitachi TM3000 tabletop scanning electron microscope (SEM) equipped with energy

dispersive spectroscopy (EDS) (Hitachi TM3000, Japan). This categorization provided input for model development discussed later in this paper.

Model validity was assessed using Method A of ASTM C1285 (the Product Consistency Test, or PCT)(16). Under this method, triplicate samples of select glasses were analyzed alongside the Approved Reference Material (ARM-1) glass(17) and blanks, to quantify chemical durability. Glass samples were ground, washed, and prepared according to the standard procedure(16). Fifteen milliliters of Type-I ASTM water were added to approximately 1.5 grams of glass in stainless steel vessels. The vessels were closed, sealed, and placed in an oven at 90 ± 2°C where they were maintained at temperature for 7 days (+/-2%). The vessels were then removed from the oven and cooled to ambient temperature. Once cooled, the leachate solution from each vessel was sampled (filtered and acidified) and analyzed by ICP-AES. Samples of a multi-element standard solution were included alongside the leachate samples to check the accuracy of the ICP-AES instrument. Normalized concentrations were calculated using the targeted glass compositions.

3 Results and Discussion

Visual observations and EDS analyses were used to categorize the crystalline content in the heat-treated glasses. Heat-treated glasses generally displayed one of four types of crystallization: no observable crystallization, minimal crystallization with spinel constituting the primary crystalline phase, bulk crystallization that included a substantial quantity of a sodium aluminosilicate (such as nepheline), and bulk crystallization where a sodium aluminosilicate phase was not present. Crystallization occurring only at the surface, reported for similar glass compositions(13, 18, 19), was not observed in these study glasses. The lack of surface crystallization in the present glasses can likely be attributed to spinel crystals in the bulk glass serving as nucleation sites, as spinel was not reported in the earlier studies. A representative image of a glass from each category is shown Figure 3.

Crystalline phase determinations were made from gross EDS analyses and knowledge of the glass system. While it is recognized that some of the crystalline phases that precipitate in waste glasses can accommodate substitutional or secondary constituents, the phase determinations in this work are consistent with literature and are only provided here due to the historical relationship between the observed presence of nepheline crystals and reduced glass durability. However, while the presented model derivation (discussed below) considers how the glass structure could be affected by select crystalline phases known to form in nuclear waste type glasses, it is ultimately the calculated residual glass strength that this paper proposes as the critical factor in predicting durability. Because of

this, the actual crystalline phases that may or may not be present after slow cooling in the test glasses are not considered in the SIR glass model since they do not influence the final results. Primary crystalline constituents determined via EDS analysis are also provided in Figure 3.

Based on known glass composition and observed crystallinity, an approach was taken to develop a method for evaluating whether the reduction in glass durability, associated with nepheline crystallization, could be successfully pre-determined. To accomplish this, several criteria were initially proposed for screening glasses. These criteria included ensuring that (1) the parent glass viscosity is sufficiently low to facilitate pouring, (2) Al_2O_3 is the limiting factor for nepheline crystallization (i.e., the residual glass post-nepheline crystallization will still contain alkali and SiO_2), (3) excess boron is not added to the system which would ultimately limit waste loading (since boron is not a primary component of the waste stream, its addition to the concentrations seen in the glass composition can only come from glass forming chemicals and cannot possibly increase waste loading, making it a limiting factor), and (4) the residual glass would have enough SiO_2 to maintain its structure and chemical durability post-crystallization, as determined by calculating a non-bridging oxygen (NBO) based ratio.

To satisfy the first criterion, a NBO-like ratio based on previous work for similar glasses(19-21) was calculated from the molar concentrations of oxides in the test glasses, according to Equation 2, where RO_x is equivalent to the sum of all components listed in Table 1 excluding Al_2O_3, B_2O_3, TiO_2, ZrO_2, and SiO_2. Glasses with a NBO-based ratio less than 0.55 were empirically categorized to be too viscous to facilitate pouring from a prototypic waste glass melter based on visual observations made during glass fabrication. The authors note that additional testing to confirm the applicability of this cut-off value may be warranted.

$$NBO = \frac{2(RO_x - Al_2O_3) + B_2O_3 + TiO_2 - ZrO_2}{SiO_2} \qquad (2)$$

To satisfy the remaining criteria, targeted glass compositions were modified by subtracting elements associated with crystalline phases known to precipitate in waste glasses to produce theoretical residual glass compositions. This was done to account for alteration of the residual glass as crystallization proceeds. Only crystalline phases that have been repeatedly reported to form during devitrification of nuclear waste type glasses were considered. As shown elsewhere(22-24), spinel crystals comprised of Fe, Cr, Ni, and Mn are routinely the first species to form during devitrification. However, since their formation doesn't present a deleterious influence on glass durability(25), their constituents were presumed to remain in the residual glass. Alkali-aluminosilicate minerals (such as nepheline and eucryptite) have also been shown to precipitate rapidly(18, 26), but the presence of B_2O_3 can suppress their

formation(6, 7). To account for this, a nepheline propensity term was derived by subtracting the moles of B_2O_3 from the moles of Al_2O_3 in the base glass, and equating this value to the quantity of alkali-aluminosilicate (with preference given to the larger cations for filling the alkali role based on previous research(27)), as shown in Equation 3. A one-to-one molar ratio of Al_2O_3 to B_2O_3 was selected as a reference point to coincide with both the potential formation of $Na_2Al_2B_2O_7$ glass network clusters and potential substitution of boron for aluminum to create malinkoite-like clusters ($NaBSiO_4$). The rationale behind this being that specific grouping/linkage of atoms may be more (or less) resistant to crystal formation in a glass system. This one-to-one molar ratio also coincides with a recent study that showed the replacement of Si-O-Al with Si-O-B linkages suppresses nepheline crystallization(28). For glasses that contained excess boron (i.e., the parent glass had a higher molar concentration of B_2O_3 than Al_2O_3), the nepheline propensity term was set to zero.

$$(K,Na,Li)AlSiO_4 = 2(Al_2O_3\text{-}B_2O_3) \quad (3)$$

The remaining alkali, or total alkali for glasses with excess B_2O_3, were then presumed to sequester to a metasilicate phase since these crystals have been commonly reported to be present alongside nepheline(9, 19, 23, 29-32). While lithium silicate crystallization has been reported to have a minimal impact on glass durability (4), it does remove SiO_2 from the residual glass, making it worth consideration. The remaining oxides were assumed to constitute an alkali-free residual glass composition containing a molar ratio of B_2O_3 to Al_2O_3 greater than or equal to one. The non-bridging oxygen ratio of this residual glass was calculated according to Equation 2. Compositions that produced a NBO value greater than 4 were removed from modeling consideration since this indicated that there was too little silica in the residual glass to maintain a cohesive structure post crystallization. While not physically possible, negative NBO values were allowed, since it was assumed that this could be an indication that additional crystalline phases such as various pyroxenes form.

The glasses that satisfied these criteria (33 out of 50), as well as the 4 glasses that satisfied all criteria other than the viscosity related term, were plotted on a ternary diagram with the calculated moles of $(K,Na,Li)AlSiO_4$, $(Li,Na)_2SiO_3$, and oxides in the residual glass at the vertices, shown in Figure 4. Molar ratios representing the relative quantity of each vertex for glasses lying inside the ternary (i.e., glasses with a higher molar concentration of Al_2O_3 than B_2O_3) can be expressed according to Equations 4 through 6, where MO_x represents the total moles of oxide present in the parent glass composition. An example calculation is provided in supplemental data.

$$(K,Na,Li)AlSiO_4 = \frac{2(Al_2O_3 - B_2O_3)}{MO_x - Al_2O_3 + B_2O_3 - K_2O - Li_2O - Na_2O} \quad (4)$$

$$(Li,Na)_2SiO_3 = \frac{Li_2O+Na_2O+K_2O-Al_2O_3+B_2O_3}{MO_x-Al_2O_3+B_2O_3-K_2O-Li_2O-Na_2O} \quad (5)$$

$$Residual = \frac{MO_x-2(Al_2O_3-B_2O_3+K_2O+Li_2O+Na_2O)}{MO_x-Al_2O_3+B_2O_3-K_2O-Li_2O-Na_2O} \quad (6)$$

In addition to providing a new visual aid for the glass compositions, the ternary effectively provides insight on the processing and crystallization behavior of a glass. Glasses lying close to the (K,Na,Li)$AlSiO_4$ vertex would generally be expected to be more refractory, and are simultaneously high in Al_2O_3 and low in B_2O_3, indicating that more nucleation sites for nepheline may exist, or at a minimum, a shorter diffusion path for crystal growth exists (since the previously stated criteria ensured the Al_2O_3 concentration was the limiting factor). In comparison, glasses lying close to the $(Li,Na)_2SiO_3$ vertex would be expected to be more fluid due to the relatively high concentration of alkali, which likely aids in the rate of diffusion for crystal growth (33, 34) and contributes to a decrease in glass durability. Glasses lying close to the residual glass vertex and on the $(Li,Na)_2SiO_3$-Residual tie-line have a higher concentration of B_2O_3 and would be expected to be more resilient to nepheline crystallization. The presence of SiO_2 in all vertices may also help to explain why its inclusion in a simple linear descriptor decreased the descriptor's accuracy(11). In addition, substitution of other species such as Fe and Ca into the nepheline phase, as reported elsewhere(27), is not anticipated to have a large impact on this model since the residual glass would still contain the same number of moles.

As shown in Figure 4, the glasses that displayed only spinel crystallization generally have a relatively low concentration of calculated metasilicate, while the glasses that showed nepheline crystallization had a comparatively high concentration of alkali, consistent with previous research(11). In addition, glasses that satisfied all criteria other than the viscosity term are comparatively high in calculated (K,Na,Li)$AlSiO_4$ and low in calculated metasilicate. These observations allowed for a new composition region where nepheline doesn't readily form, illustrated by the orange dotted line in Figure 4 and corresponding to the ratio presented in Equation 7, to be realized.

$$\frac{(Li,Na)_2SiO_3}{(Li,Na)_2SiO_3+Residual} \leq 0.31 \quad (7)$$

The 12 glasses that simultaneously fell above this line and were determined not to have excess B_2O_3 were subjected to a product consistency test(16) to determine whether the glasses exhibited acceptable chemical durability. The results revealed that 10 out of the 12 glasses displayed leaching rates lower than those of the reference Environmental Assessment (EA) glass(35). The 2 glasses that exhibited higher leaching rates did not satisfy the viscosity criteria specified previously, and formed additional crystalline species presumed to be damaging to durability (i.e., mullite/cristobalite), shown in Figure 3d.

To confirm the applicability of this model, glasses previously developed and studied by Kroll et.al,(29, 36) were put through the same screening process. Of the 57 glasses screened, 48 were determined to be suitable for modeling, 25 fell above the 0.31 line, 24 did not have excess B_2O_3, and 10 simultaneously fell in the region proposed to be chemically durable, resilient to nepheline crystallization, and didn't have excess B_2O_3, as shown in Figure 5.

Additional investigation into the glasses that fell above the 0.31 ratio line provided further confidence in the model's ability to accurately screen select glass compositions for both formation of nepheline crystallization and acceptable durability since 20 out of 25 displayed nepheline crystallization less than 7 wt% (a concentration demonstrated to be acceptable(4)) and 21 out of the 25 displayed significantly lower leaching rates than those of the benchmark EA glass(35). In addition, a structural dependency on the previously calculated NBO value for the residual glass for both the observed quantity of nepheline crystallization and measured PCT response after being subjected to a canister centerline cooling (CCC) heat treatment was revealed, as shown in Figure 6.

The decrease in durability as the NBO value increases above 3 is consistent with previous work (13) that showed an increase in boron leaching as the residual glass structure was diminished. In addition, a NBO value less than zero is not physically possible, and is attributed to high Al_2O_3/SiO_2 ratios in the residual glass. This concentration likely forces Al_2O_3 to adopt a different structural role, or to precipitate additional crystalline phases (such as combining with the metasilicate to form additional nepheline-like phases, or various pyroxenes and spinels) that in return diminish durability. To accommodate this observation, the previous screening criterion that the NBO-based ratio of the residual glass must be less than 4 was replaced with the criterion that the NBO must be between -1 and 3.

This new screening criterion was utilized to further investigate the study glasses presented here as well as the 57 Kroll glasses(29, 36). The glass compositions were compared to measured boron leaching results and divided into sub-groups to highlight the model's efficiency. As shown in Table 2, the model accurately categorized 53 out of the 69 glasses for acceptable durability. These results indicate that a misclassification rate of ~23% exists. While this value may be higher than ideal, it is better than reported values for other nepheline models(11, 14), maintains a conservative approach to avoid producing false negatives (i.e., 100% of glasses predicted to be durable exhibited acceptable leaching), and focuses on maintaining glass durability as opposed to suppressing crystal formation. This last point is especially important for allowing access to new glass composition regions, since chemical durability is the most important long-term factor, and previous studies have shown that some degree of nepheline crystallization is not necessarily prohibitive(4, 13). It should also be noted that the misclassification rate could be improved to ~16%

by only relying on the calculated NBO value, but comes at the expense of conservatism by increasing the percent of false negatives from 0% to ~7%.

Since the model is dependent on maintaining certain ratios between glass components, a relatively wide range of glass compositions can be accessed under the proposed modeling criteria. The concentrations of the major components in the 29 glasses predicted and proven to be durable are shown in Figure 7. Also shown in Figure 7 is an apparent inverse relationship between B_2O_3 and SiO_2, presumably because they both play a substantial role in maintaining the glass structure. In addition, the glasses contain between 20-35 wt% Al_2O_3, matching the previously highest reported values achieved(11), and are consistent with a waste loading in excess of 36 wt% for Al_2O_3 limited waste streams. In fact, the Na_2O concentration is more likely to be the limiting factor in this model, although this can be alleviated by modifying the concentration of Li_2O added.

Comparison between the current study (Structural Integrity of Residual model) and other nepheline discriminators is given in Table 3. As shown in the table, the new SIR model allows for both the highest allowable Al_2O_3 waste loading and achieved zero false negatives (albeit on a reduced sample population). While additional work is needed to determine the confidence limits associated with this model, as well as to determine whether the formation/quantity of spinel crystal phases is acceptable for processability (i.e., every glass shown to be durable had some quantity of spinel crystals present), it does open a distinct glass composition region that cannot be accessed under the current ND. In addition, the model appears to be able to adequately screen glasses for acceptable leaching behavior, offering a new method to enhance waste loading.

4 Summary

An approach was taken to develop a new model based on targeted glass compositions and glass structure to allow for enhanced Al_2O_3 waste loading in nuclear waste glass while maintaining chemical durability. In contrast to the historical approach of correlating durability to the presence or accumulation of specific phases (e.g., nepheline) in the glass, this new model proposes a more universal concept that the residual glass composition is the critical factor that determines glass durability. In addition, the calculated non-bridging oxygen content in the theoretical residual glass was demonstrated to successfully screen glasses for acceptable durability since glasses with NBO values between -1 and 3 generally displayed leaching substantially lower than the reference EA glass. While additional testing to ensure the quantity of spinel crystallization allowed does not inhibit processability, the newly proposed SIR model was shown to allow for both the highest reported Al_2O_3 waste loading and achieve the lowest amount of false negatives

when compared to analogous models. These results provide a new technique to aid in optimizing nuclear waste vitrification.

Acknowledgements

This work was supported by the U.S. Department of Energy Office of River Protection Waste Treatment & Immobilization Plant Project. Savannah River National Laboratory is operated by Savannah River Nuclear Solutions for the U.S. Department of Energy under contract number DE-AC09-08SR22470.

References

1. Harp BJ, Noyes DL, Trenchard GD, Hamel WF. River Protection Project System Plan. U.S. Department of Energy Office of Reiver Protection, 2017 Report No.: ORP-11242, Rev 8.

2. Peeler DK, Kim DS, Vienna JD, Schweiger MJ, Piepel GF. Office of River Protection Advanced Low-Activity Waste Glass Research and Development Plan. Richland, WA: Pacific Northwest National Laboratory, 2015 Report No.: PNNL-24883.

3. Vienna J, Kim D, Schweiger M, Piepel G, Kroll J, Kruger A. Glass Formulation and Testing for U.S. High-Level Tank Wastes Project 17210 Year 1 Status Report: October 15, 2014. 2014 Report No.: PNNL-SA-84872.

4. Kim D-S, Peeler DK, Hrma P. Effect of Crystallization on the Chemical Durability of Simulated Nuclear Waste Glass. American Ceramic Society; Cincinnati, OH1995. p. 177-86.

5. Jantzen CM, Bickford DF. Leaching of Devitrified Glass Containing Simulated SRP Nuclear Waste. MRS Proceedings. 1984;44:135-46.

6. Fox KM, Edwards TB, Peeler DK. Control of Nepheline Crystallization in Nuclear Waste Glass. International Journal of Applied Ceramic Technology. 2008;5(6):666-73.

7. Li H, Hrma P, Vienna JD, Qian M, Su Y, Smith DE. Effects of Al2O3, B2O3, Na2O, and SiO2 on nepheline formation in borosilicate glasses: chemical and physical correlations. Journal of Non-Crystalline Solids. 2003;331(1):202-16.

8. Li H, Vienna J, Hrma P, Smith D, Schweiger M. Nepheline Precipitation in High-Level Waste Glasses : Compositional Effects and Impact on the Waste Form Acceptability. MRS Proceedings. 1996;465.

9. Rodriguez C, McCloy J, Schweiger M, Crum J, Winschell A. Optical Basicity and Nepheline Crystallization in High Alumina Glasses. Richland, WA: Pacific Northwest National Laboratory, 2011 Report No.: PNNL-20184.

10. Vienna JD, Kroll JO, Hrma PR, Lang JB, Crum JV. Submixture model to predict nepheline precipitation in waste glasses. International Journal of Applied Glass Science. 2017;8(2):143-57.

11. Sargin I, Lonergan CE, Vienna JD, McCloy JS, Beckman SP. A Data-Driven Approach for Predicting Nepheline Crystallization in High-Level Waste Glasses. Journal of the American Ceramic Society. 2020.

12. Vienna JD, Kim D-S, Skorski DC, Matyas J. Glass Property Models and Constraints for Estimating the Glass to be Produced at Hanford by Implementing Current Advanced Glass Formulation Efforts. Richland, WA: Pacific Northwest National Laboratory, 2013 Report No.: PNNL-22631, Rev. 1.

13. McClane DL, Amoroso JW, Fox KM, Hsieh MC, Kesterson MR, Kruger AA. Nepheline Crystallization and the Residual Glass Composition: Understanding Waste Glass Durability. International Journal of Applied Glass Science. 2020.

14. Goel A, McCloy J, Pokorny R, Kruger A. Challenges with vitrification of Hanford High-Level Waste (HLW) to borosilicate glass – An overview. Journal of Non-Crystalline Solids. 2019;4.

15. Pareizs J, Billings A, Reboul S, Lambert D, Click D. Sludge Batch 7b Qualification Activities With SRS Tank Farm Sludge. Aiken, SC: Savannah River National Laboratory, 2011 Report No.: SRNL-STI-2011-00548, Rev. 0.

16. ASTM C1285-14, Standard Test Methods for Determining Chemical Durability of Nuclear, Hazardous, and Mixed Waste Glasses and Multiphase Glass Ceramics: The Product Consistency Test (PCT). West Conshohocken, PA2014.

17. Jantzen CM, Pickett JB, Brown KG, Edwards TB, Beam DC. Process/Product Models for the Defense Waste Processing Facility (DWPF): Part I. Predicting Glass Durability from Composition Using a Thermodynamic Hydration Energy Reaction Model (THERMO). Aiken, SC: Westinghouse Savannah River Company, 1995 WSRC-TR-93-672, Revision 1.

18. Marcial J, Neill OK, Newville M, Crum JV, McCloy J. Effect of cooling profile on crystalline phases, oxidation state, and chemical partitioning of complex glasses. MRS Advances. 2020:1-11.

19. McClane DL, Amoroso JW, Fox KM, Kruger AA. Nepheline crystallization behavior in simulated high-level waste glasses. Journal of Non-Crystalline Solids. 2019;505:215-24.

20. Jantzen C, Edwards T. Defense Waste Processing Facility (DWPF) Viscosity Model: Revisions for Processing High TiO_2 Containing Glasses. Savannah River Site (SRS), 2016.

21. White WB, Minser DG. Raman spectra and structure of natural glasses. Journal of Non-Crystalline Solids. 1984;67(1):45-59.

22. Lonergan CE, Akinloye-Brown K, Rice J, Gervasio V, Canfield N, Schweiger MJ, et al. Micron-sized spinel crystals in high level waste glass compositions: Determination of crystal size and crystal fraction. Journal of Nuclear Materials. 2019;514:196-207.

23. Cicero CA, Marra SL, Andrews MK. Phase Stability Determinations of DWPF Waste Glasses (U). Aiken, SC: Westinghouse Savannah River Co., 1993 Report No.: WSRC-TR-93-227, Rev. 0.

24. Christian JH. Crystallization in high-level waste glass: A review of glass theory and noteworthy literature. Aiken, SC: Savannah River National Laboratory, 2015.

25. Bickford DF, Jantzen CM. Devitrification Behavior of SRL Defense Waste Glass. MRS Proceedings. 1983;26:557.

26. Menkhaus T, Hrma P, Li H. Kinetics of Nepheline crystallization from high-level waste glass. Ceramic Transactions. 2000:461-8.

27. Marcial J, Crum J, Neill O, McCloy J. Nepheline structural and chemical dependence on melt composition. American Mineralogist. 2016;101(2):266-76.

28. Deshkar A, Gulbiten O, Youngman R, Mauro J, Goel A. Why does B2O3 suppress nepheline (NaAlSiO4) crystallization in sodium aluminosilicate glasses? Physical Chemistry Chemical Physics. 2020;22.

29. Kroll J, Vienna J, Schweiger MJ, Piepel G, Cooley S. Results from Phase 1, 2, and 3 Studies on Nepheline Formation in High-Level Waste Glasses Containing High Concentrations of Alumina. Richland, Washington: Pacific Northwest National Laboratory, 2016 Report No.: PNNL-26057, Rev 0.

30. Fox KM, Peeler DK, Edwards TB. Nepheline Crystallization in Nuclear Waste Glasses. Advances in Materials Science for Environmental and Nuclear Technology. 2010;222:77-90.

31. Fox K, Edwards T. Experimental Results Of The Nepheline Phase III Study. ; SRS, 2009 SRNL-STI-2009-00608; TRN: US1000081 United States 10.2172/969038 TRN: US1000081 available SRS English.

32. Fox K, James Newell J, Tommy Edwards T, David Best D, Irene Reamer I, Phyllis Workman P. Refinement Of The Nepheline Discriminator: Results Of A Phase I Study. Aiken, SC: Savannah River National Laboratory, 2008 2008-02-13. Report No.: Report No.: WSRC-STI-2007-00659.

33. Zwanzig R. On the relation between self-diffusion and viscosity of liquids. J Chem Phys 1983;79(9):4507-8.

34. Nascimento MLF, Zanotto ED. Does viscosity describe the kinetic barrier for crystal growth from the liquidus to the glass transition? The Journal of Chemical Physics. 2010;133(17):174701.

35. Jantzen CM, Bibler NE, Beam DC, Crawford CL, Pickett MA. Characterization of the Defense Waste Processing Facility (DWPF) Environmental Assessment (EA) Glass Standard Reference Material (U). Aiken, SC: Westinghouse Savannah River Co., 1993 Report No.: WSRC-TR-92-346, Rev. 1.

36. Kroll JO, Vienna JD, Nelson ZJ, Skidmore CH. Results from Phase 5 Study on Nepheline Formation in High-Level Waste Glasses Containing High Concentrations of Alumina. Richland, Washington: Pacific Northwest National Laboratory, 2018 Report No.: PNNL-27555.

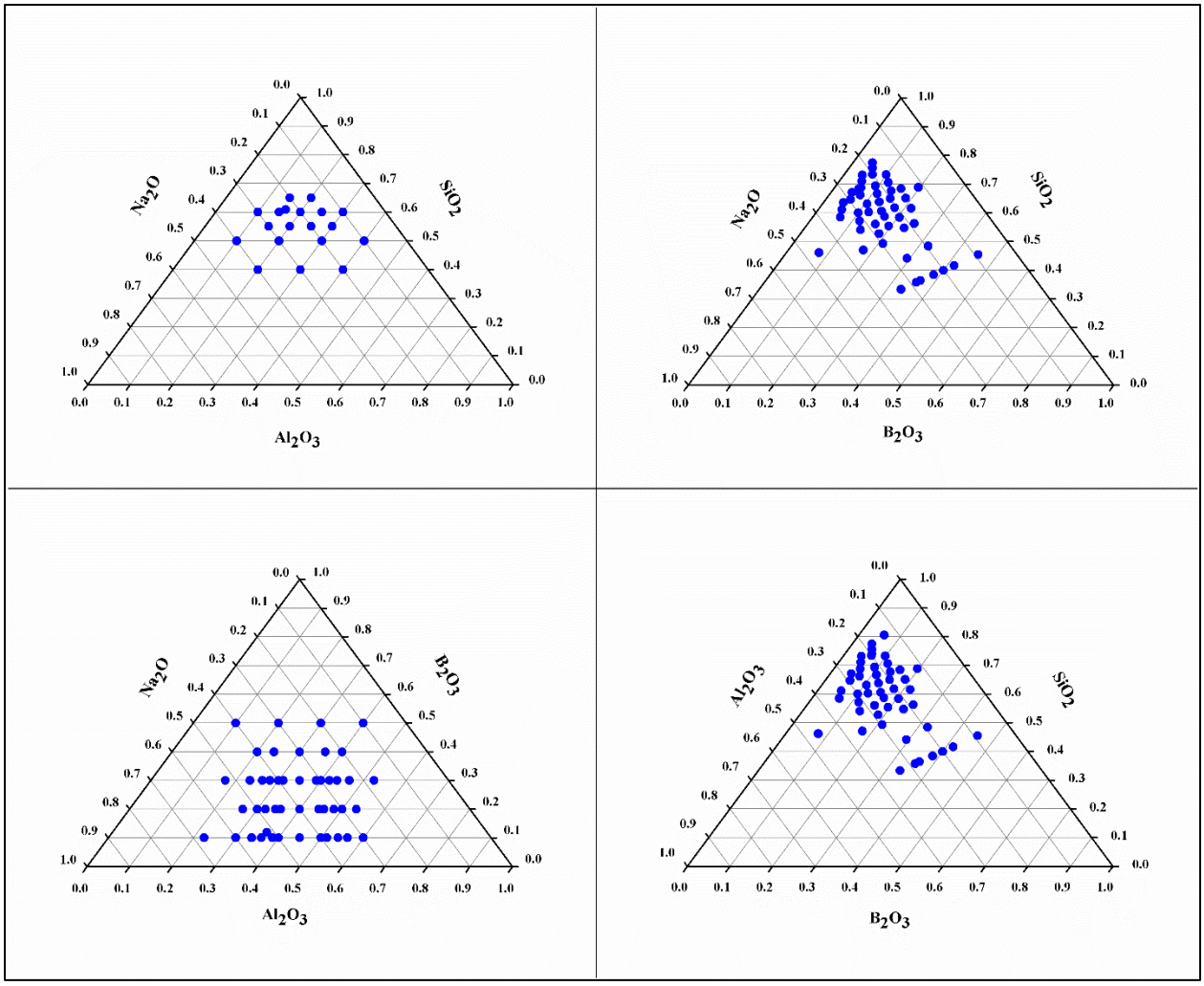

Figure 1: Molar ratios between major components in study glasses

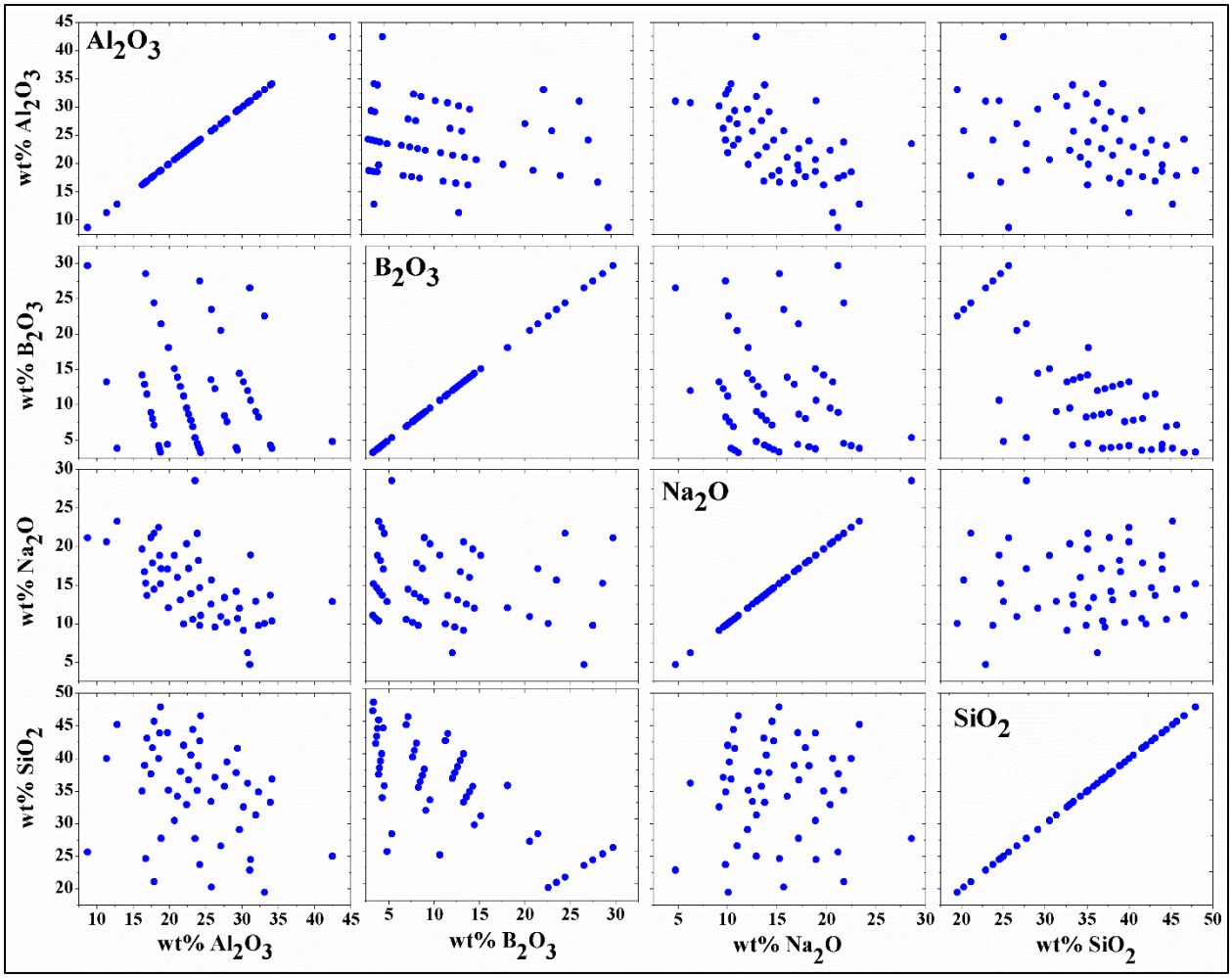

Figure 2: Weight percent of Al_2O_3, B_2O_3, Na_2O, and SiO_2 in investigated glasses

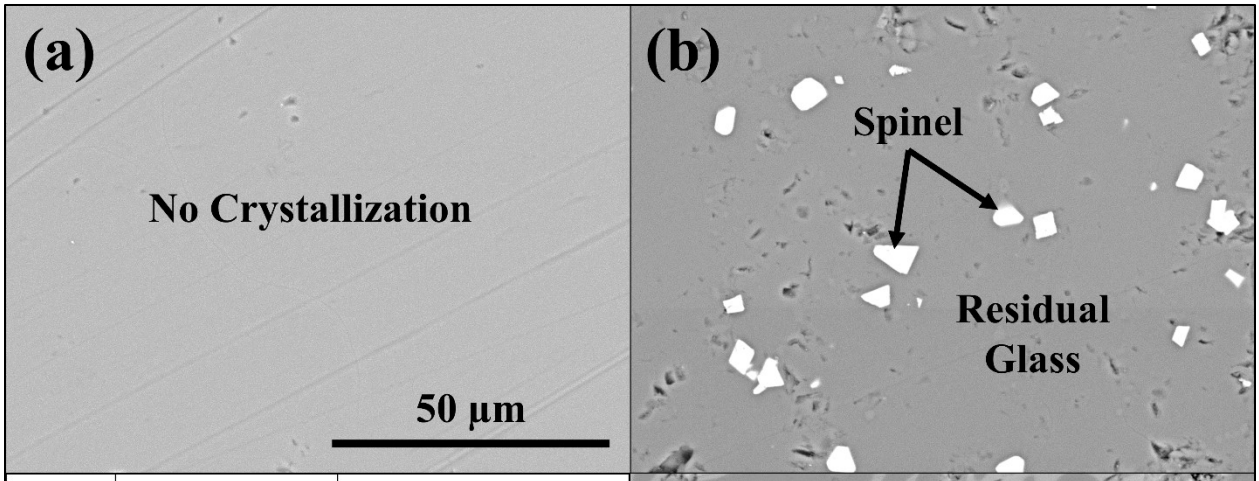

Image	Phase Identified	Primary Constituents[1]
(a)	Glass	Al, Na, Si, O
(b)	Residual Glass	Al, Na, Si, O
	Spinel	Cr, Fe, O
(c)	Residual Glass	Na, Si, O
	Nepheline[2]	Al, Na, Si, O
	Lithium Silicate	Si, O
	Spinel	Cr, Fe, O
	P-Rich Phase[3]	Al, Ca, Na, P, Si, O
(d)	Residual Glass	Al, Na, Si, O
	Mullite[4]	Al, Si, O
	Spinel	Cr, Fe, O

[1] Note that B & Li can't be detected with EDS

[2] Ratio of Na/Al/Si agrees with Nepheline phase

[3] Presumed to be calcium apatite

[4] Assumed to be mullite/cristobalite solid solution

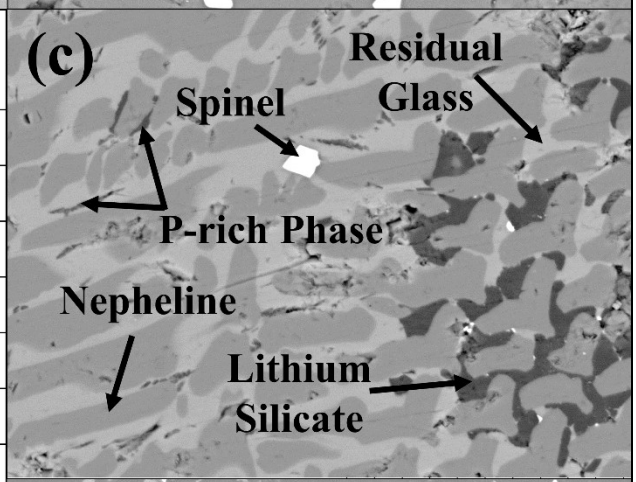

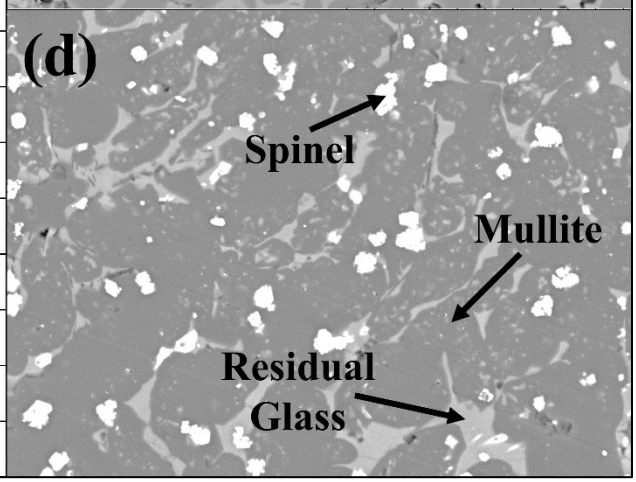

Figure 3: Images of crystallization observed in typical study glasses and major constituents observed in phases identified via EDS analysis

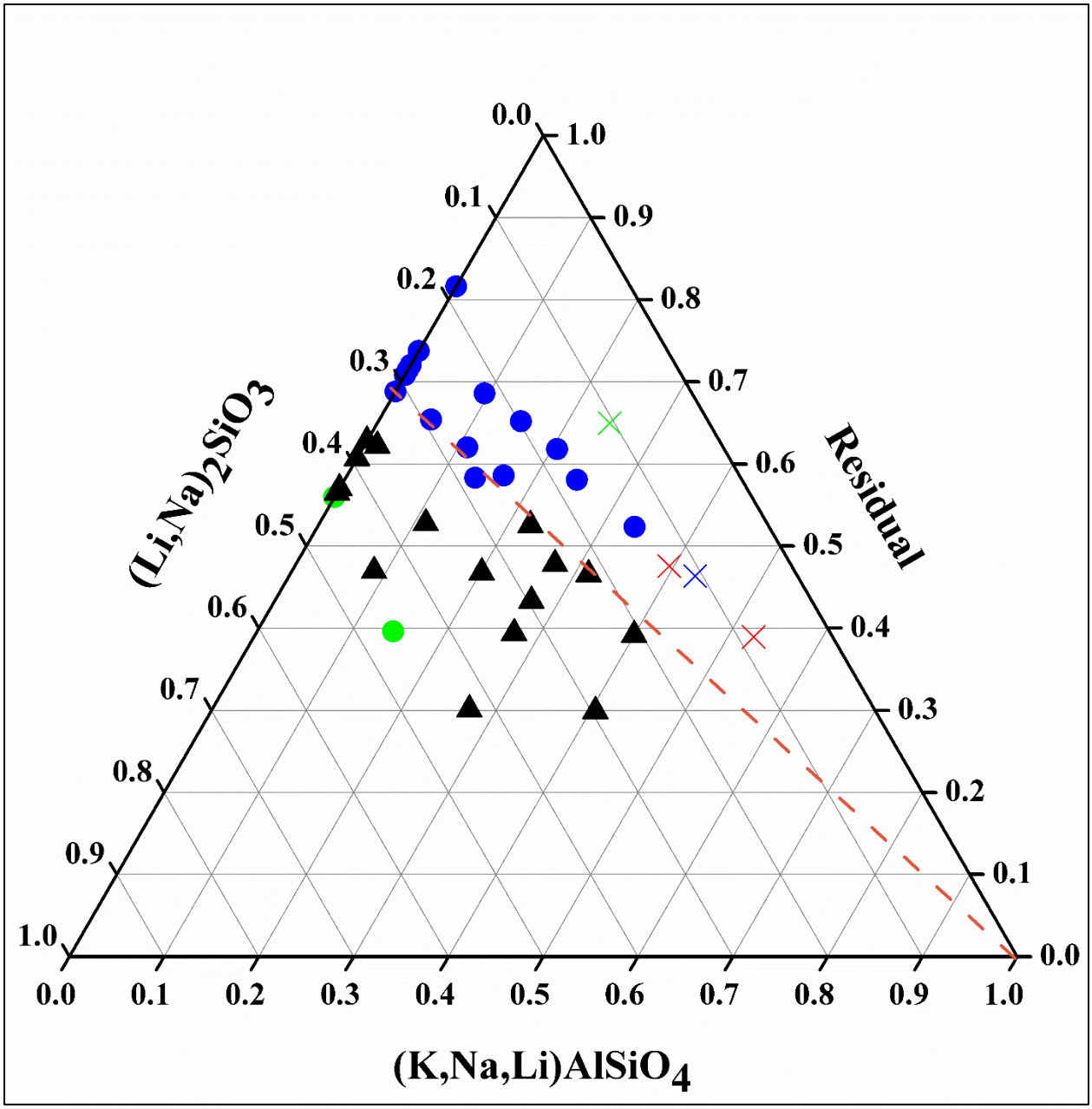

Figure 4: Ternary diagram showing calculated molar ratios of SIR glasses that satisfied modeling criteria. Green symbols indicate no crystallization observable, blue symbols indicate spinel is primary crystalline phase, black symbols indicate bulk nepheline crystallization observed, red symbols indicate bulk crystallization without nepheline, and Xs mark compositions screened out by viscosity criterion.

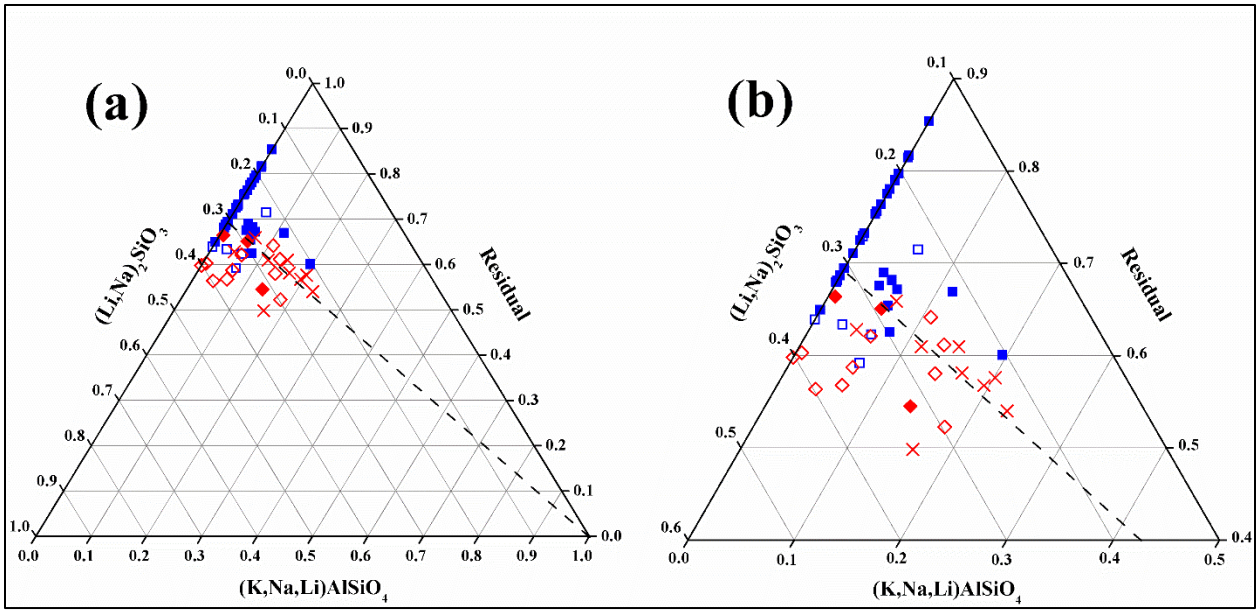

Figure 5: (a) Full ternary diagram and (b) Partial ternary diagram showing calculated molar ratios of glasses from previous studies(29, 36), where blue symbols represent durable glasses, red symbols represent glasses with leaching values higher than the EA glass[29], solid symbols represent glasses with a residual NBO between -1 and 3, open symbols represent glasses with a residual NBO greater than 3 or less than -1, and Xs represent compositions with no SiO_2 in the residual.

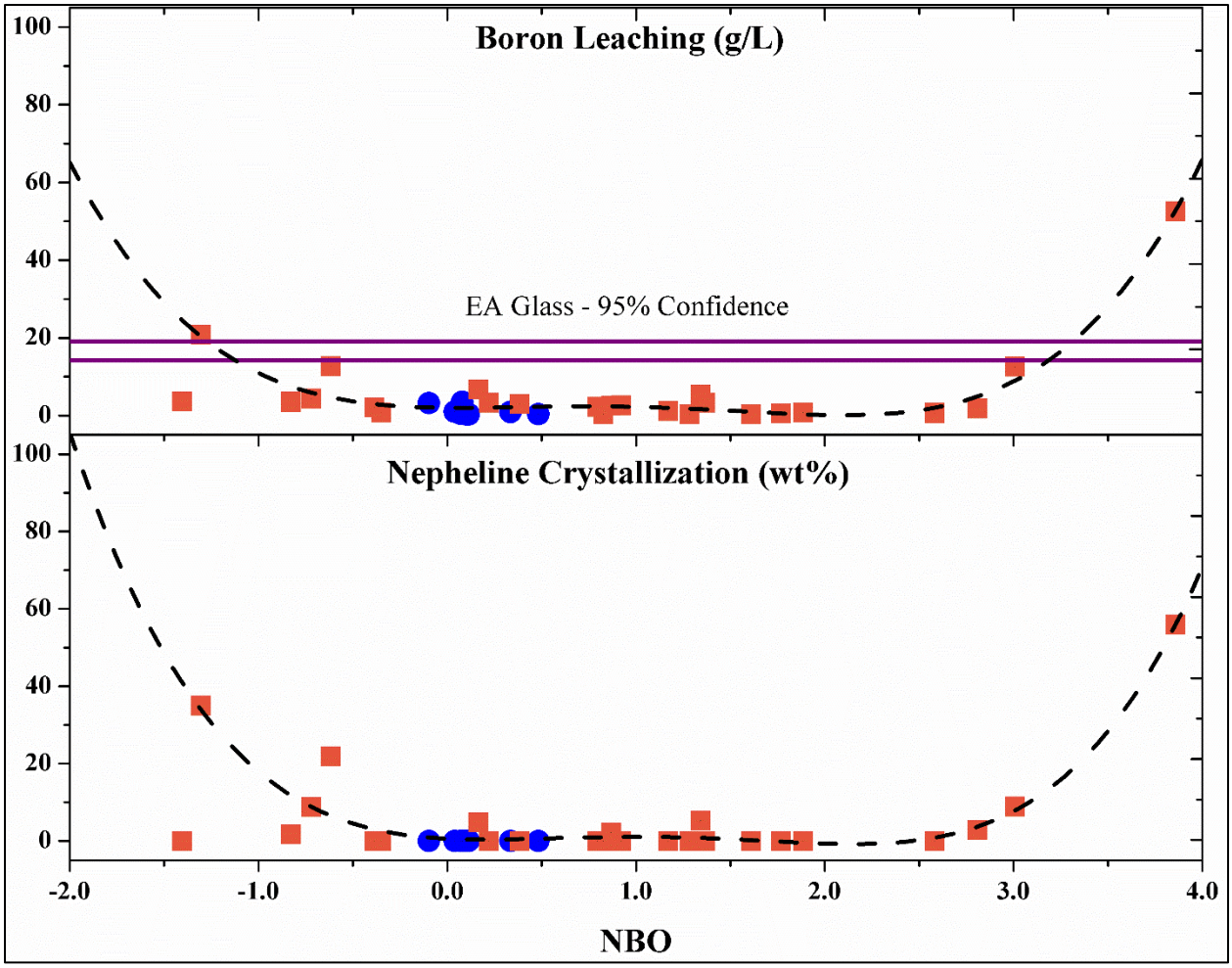

Figure 6: Measured nepheline concentrations and boron release from heat treated glasses from the current study (blue circles) and References (29, 36) (orange squares) as a function of 'Residual Glass' NBO value.

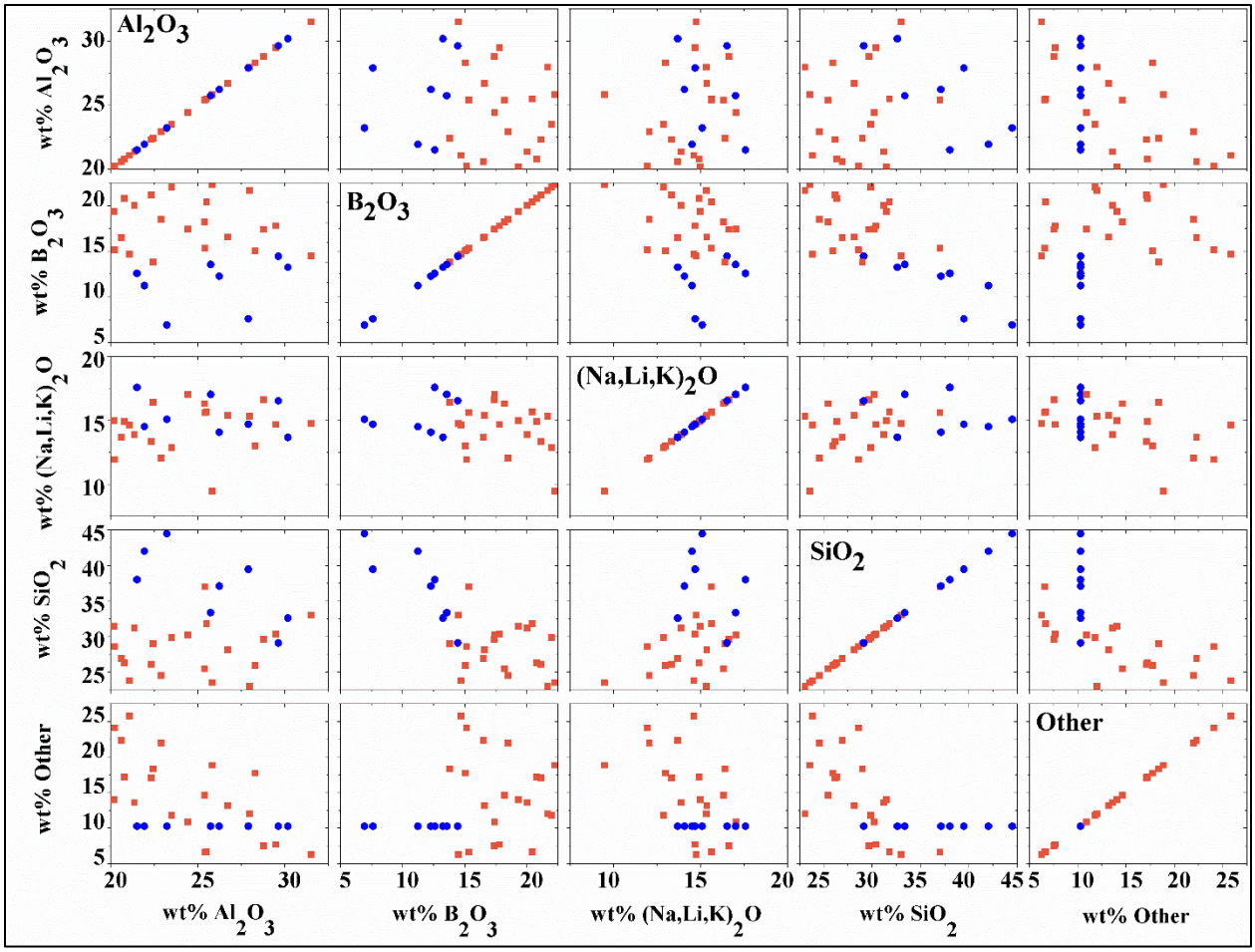

Figure 7: Weight percent of major components in glasses from the current study (blue circle) and References (29, 36) (orange square) that fit modeling requirements for acceptable durability.

Table 1: Representative waste compositions(14) and concentration of components in test glasses.

Component	Al-Limited (wt%)	Al & Na Limited (wt%)	Maximum Concentration from Waste Stream for Glass Containing 36 wt% Waste Loading (wt%)	Moles per Gram of Glass	Concentration of Components in Study Glasses (wt%)
Al_2O_3	52.95	45.13	19.06	1.87E-03	8.70 – 42.45
B_2O_3	0.42	0.77	0.28	3.98E-05	3.23 – 29.71
BaO	0.12	0.06	0.04	2.82E-06	-
Bi_2O_3	2.53	2.45	0.91	1.95E-05	0.91
CaO	2.38	1.53	0.86	1.53E-04	0.86
CdO	0.05	0.02	0.02	1.40E-06	-
Cr_2O_3	1.15	1.50	0.54	3.55E-05	0.54
Cs_2O_3	0.50	0.50	0.18	5.74E-06	-
F	1.47	0.48	0.53	2.79E-04	0.53
Fe_2O_3	13.03	5.95	4.69	2.94E-04	4.69
K_2O	0.31	1.40	0.50	5.35E-05	0.50
Li_2O	0.38	0.16	0.14	4.58E-05	4.00
MgO	0.26	0.46	0.17	4.11E-05	0.17
Na_2O	7.91	26.88	9.68	1.56E-03	4.72 – 28.60
NiO	0.88	0.21	0.32	4.24E-05	0.32
P_2O_5	2.32	4.27	1.54	1.08E-04	1.54
PbO	0.90	0.19	0.32	1.45E-05	-
RuO_2	0.10	0.10	0.04	2.71E-06	-
SiO_2	10.81	6.48	3.89	6.48E-04	19.49 – 47.91
SO_3	0.44	0.46	0.17	2.07E-05	0.17
TiO_2	0.02	0.36	0.13	1.62E-05	0.13
ZnO	0.18	0.38	0.14	1.68E-05	0.14
ZrO_2	0.87	0.26	0.31	2.54E-05	0.31

Table 2: Dependency of Model Accuracy on Various Screening Parameters

Glasses	Model	NBO	Location on Ternary	Prediction	Quantity of Glasses with Leaching Rates Lower than EA(35)	Quantity of Glasses with Leaching Rates Higher than EA(35)	SIR Model Accuracy
Kroll(29,36)	No[1]	n/a	n/a	Not Durable	0	9	100%
	Yes	NBO>3 or NBO<-1	Below 0.31 Ratio Line	Not Durable	4	8	67%
			Above 0.31 Ratio Line	Not Durable	2	2	50%
		-1<NBO<3	Below 0.31 Ratio Line	Not Durable	8	3	27%
			Above 0.31 Ratio Line	Durable	21	0	100%
This Study	No[2]	-1<NBO<3	Above 0.31 Ratio Line	Not Durable	2	2	50%
	Yes	-1<NBO<3	Above 0.31 Ratio Line	Durable	8	0	100%

[1]Insufficient SiO_2
[2]Viscosity criterion not met

Table 3: Comparison between nepheline discriminator models(10-12, 14)

	ND	ND + OB	NN	SM – Conservative	DC	SIR (Current Study)
True Positives	206	192	147	402	161	29
False Positives	273	206	32	133	67	16
True Negatives	268	335	439	212	473	24
False Negatives	0	14	11	0	53	0
Total	747	747	629	747	754	69
Maximum Reported Al_2O_3 (wt%)	18	24	28	27	32	32
False Negatives (%)	0.0%	1.9%	1.7%	0.0%	7.0%	0.0%

Supplemental Data

Table S1: Concentration (wt%) of major components in study glasses

Glass ID	Al_2O_3	B_2O_3	Na_2O	SiO_2
SIR-1	8.70	29.71	21.16	25.64
SIR-2	11.31	13.24	20.63	40.01
SIR-3	23.52	5.35	28.60	27.73
SIR-4	17.90	24.44	21.76	21.10
SIR-5	23.83	4.52	21.73	35.12
SIR-6	22.35	9.54	20.38	32.93
SIR-7	20.70	15.14	18.87	30.49
SIR-8	16.73	28.56	15.26	24.65
SIR-9	22.92	7.83	13.93	40.52
SIR-10	19.88	18.10	12.08	35.14
SIR-11	31.15	10.64	18.94	24.48
SIR-12	25.79	23.48	15.68	20.26
SIR-13	33.89	4.29	13.74	33.29
SIR-14	31.89	9.07	12.92	31.32
SIR-15	29.63	14.45	12.01	29.11
SIR-16	24.17	27.50	9.79	23.74
SIR-17	42.45	4.83	12.90	25.02
SIR-18	33.07	22.58	10.05	19.49
SIR-19	30.74	12.00	6.23	36.24
SIR-20	31.07	26.52	4.72	22.89
SIR-21	18.76	3.32	15.21	47.91
SIR-22	24.32	3.23	11.09	46.57
SIR-23	18.63	3.77	18.88	43.92
SIR-24	24.15	3.66	14.68	42.70
SIR-25	29.37	3.57	10.71	41.55
SIR-26	23.99	4.10	18.23	38.88
SIR-27	29.18	3.99	14.19	37.84
SIR-28	17.89	7.13	14.50	45.69
SIR-29	23.22	6.94	10.58	44.47
SIR-30	17.66	8.04	17.89	41.62
SIR-31	27.91	7.62	10.18	39.48
SIR-32	22.63	8.69	17.20	36.68
SIR-33	27.57	8.47	13.41	35.75
SIR-34	16.88	11.53	13.68	43.11
SIR-35	21.94	11.24	10.00	42.02
SIR-36	16.54	12.91	16.76	38.99
SIR-37	21.51	12.59	13.08	38.03
SIR-38	26.24	12.28	9.57	37.11
SIR-39	21.10	13.89	16.03	34.19
SIR-40	25.74	13.56	12.52	33.38
SIR-41	18.51	4.21	22.50	39.99
SIR-42	34.11	3.88	10.37	36.85
SIR-43	17.43	8.93	21.19	37.66
SIR-44	32.27	8.26	9.81	34.87
SIR-45	16.21	14.24	19.71	35.04
SIR-46	30.18	13.25	9.17	32.61
SIR-47	12.79	3.88	23.32	45.22
SIR-48	18.84	21.44	17.18	27.75
SIR-49	27.08	20.55	10.97	26.60
SIR-50	19.74	4.41	17.11	43.95

Example Calculation

For this example, the SIR-40 glass will be used. The glass composition presented in both weight percent and moles per 100 grams is given in Table S2 below.

Table S2: Composition of SIR-40 Glass

Component	Wt%	Mol/100g
Al_2O_3	25.74	0.2525
B_2O_3	13.56	0.1948
Bi_2O_3	0.91	0.0020
CaO	0.86	0.0153
Cr_2O_3	0.54	0.0036
F	0.53	0.0279
Fe_2O_3	4.69	0.0294
K_2O	0.50	0.0054
Li_2O	4.00	0.1339
MgO	0.17	0.0041
Na_2O	12.52	0.2020
NiO	0.32	0.0042
P_2O_5	1.54	0.0108
SiO_2	33.38	0.5555
SO_3	0.17	0.0021
TiO_2	0.13	0.0016
ZnO	0.14	0.0017
ZrO_2	0.31	0.0025

From Table S2 above, the glass composition can be simplified to the components shown in Table S3.

Table S3: Simplified Composition of SIR-40 Glass

Component	Mol/100g
Al_2O_3	0.2525
B_2O_3	0.1948
$(Li,Na,K)_2O$	0.3412
SiO_2	0.5555
TiO_2	0.0016
ZrO_2	0.0025
Other	0.1009

From Equation 2, the NBO-like ratio of the starting glass is calculated as follows:

$$NBO = \frac{2(RO_x - Al_2O_3) + B_2O_3 + TiO_2 - ZrO_2}{SiO_2}$$

$$= \frac{2(0.3412 + 0.1009 - 0.2525) + 0.1948 + 0.0016 - 0.0025}{0.5555} = 1.0 \geq 0.55$$

As shown above, the NBO-like ratio of the starting glass is greater than 0.55, indicating that it should be pourable.

The nepheline propensity term is then calculated according to Equation 3, as shown below:

$(K,Na,Li)AlSiO_4 = 2(Al_2O_3\text{-}B_2O_3) = 2(0.2525 - 0.1948) = 0.1154$

Table S4 shows the remaining glass component concentrations after this value is subtracted from the molar concentration of the simplified glass composition given in Table S3.

Table S4: Composition of SIR-40 Glass after Nepheline Propensity Calculation

Component	Mol/100g
Al_2O_3	0.1948
B_2O_3	0.1948
$(Li,Na,K)_2O$	0.2835
SiO_2	0.4401
TiO_2	0.0016
ZrO_2	0.0025
Other	0.1009

The quantity of $(Li,Na)_2SiO_3$ is then determined by assuming all of the alkali sequesters to this phase, as shown below.

$$(Li,Na)_2SiO_3 = (Li,Na,K)_2O = 0.2835$$

The final calculated residual glass composition, after the quantity of $(Li,Na)_2SiO_3$ is removed from the composition shown in Table S4, is given in Table S5.

Table S5: Residual Glass Composition of SIR-40 Glass

Component	Mol/100g
Al_2O_3	0.1948
B_2O_3	0.1948
$(Li,Na,K)_2O$	0.0000
SiO_2	0.1566
TiO_2	0.0016
ZrO_2	0.0025
Other	0.1009
Total	0.6512

The location of the glass on the ternary is determined from the calculated $(K,Na,Li)AlSiO_4$, $(Li,Na)_2SiO_3$, and total residual values above, as shown below.

$$(K,Na,Li)AlSiO_4 = \frac{(K,Na,Li)AlSiO_4}{(K,Na,Li)AlSiO_4 + (Li,Na)_2SiO_3 + Residual} = \frac{0.1154}{0.1154 + 0.2835 + 0.6512} = 0.11$$

$$(Li,Na)_2SiO_3 = \frac{(Li,Na)_2SiO_3}{(K,Na,Li)AlSiO_4 + (Li,Na)_2SiO_3 + Residual} = \frac{0.2835}{0.1154 + 0.2835 + 0.6512} = 0.27$$

$$Residual = \frac{Residual}{(K,Na,Li)AlSiO_4 + (Li,Na)_2SiO_3 + Residual} = \frac{0.6512}{0.1154 + 0.2835 + 0.6512} = 0.62$$

Since the ratio between the $(Li,Na)_2SiO_3$ and residual terms is less than 0.31, the glass is determined to fall into an area on the ternary that is anticipated to be resilient to nepheline crystallization, as shown below.

$$\frac{(Li,Na)_2SiO_3}{(Li,Na)_2SiO_3 + Residual} = \frac{0.27}{0.27 + 0.62} = 0.30 \leq 0.31$$

From Equation 2, the NBO-like ratio of the residual glass is calculated as follows:

$$NBO = \frac{2(RO_x - Al_2O_3) + B_2O_3 + TiO_2 - ZrO_2}{SiO_2} = \frac{2(0.1009 - 0.1948) + 0.1948 + 0.0016 - 0.0025}{0.1566}$$

$$= 0.04$$

As shown above, since the glass both falls above the 0.31 line and the residual glass has a NBO-like ratio between -1 and 3, the glass would be expected to be durable. PCT testing on the heat treated version of this glass revealed a normalized boron release of 1.055 g/L, significantly lower than the 16.7 g/L reported for the reference EA glass (35).